Applied Problems of Nonlinear Oscillation and Wave Theory

Izvestiya Vysshikh Uchebnykh Zavedeniy. Applied Nonlinear Dynamics. 2023;31(3)

Научная статья
УДК 519.6, 532.5

DOI: 10.18500/0869-6632-003039
EDN: HKQPIN

Article

DOI: 10.18500/0869-6632-003039

Transfer of passive particles in the velocity field of vortex tripole moving on a plane

V. N. Govorukhin

Southern Federal University, Rostov-on-Don, Russia
E-mail: vngovoruhin@sfedu.ru

Received 29.12.2022, accepted 24.03.2023,
available online 25.04.2023, published 31.05.2023

Abstract. *Purpose* of this article is to study transport processes of passive particles in the velocity field of a vortex tripole with a change in the parameter that determines the speed of the tripole movement on the plane. A structure consisting of a central vortex and satellite vortices rotating around it with the opposite vorticity is understood here as a vortex tripole. We study a system of three point vortices, the most simple mathematical representation of a vortex tripole, which expressed as a system of nonlinear ordinary differential equations with a parameter. Consideration is limited to a particular case of a tripole with zero total vorticity. The study focused on the relationship between vortex movement speed and the transport of passive particles. *Methods.* The study was performed numerically using algorithms based on the dynamical systems approaches. Its include the construction of the Poincaré map and the analysis of the dynamics of marker particles. Were carried out long times calculations, corresponding to hundreds and thousands of turns around the tripole center. High-order accuracy integrators were used to solve the Cauchy problems, allowing for better control of the calculation results.. *Results.* We discovered that the transfer of passive particles varies with vortex tripole speed.. A vast zone of chaotic dynamics forms in the neighborhood of the vortices when the velocity is low. This zone slowly shifts along with the tripole. There are subregions of active and slow mixing inside the chaos region. The possible stages of particle dynamics are: transfer from the region to the right of the tripole to the area to the left, vigorous mixing near the vortices, and slowly reverse drifting to the region to the left of the tripole. At a high speed of vortex configuration in the entire chaotic region, the particles are strongly mixed. The vortex tripole moves particles far away from where it starts and does not collect new particles along the way.. In intermediate situations, both processes can be realised at varying degrees. We have identified and discussed non-trivial scenarios for the transport of passive particles by a vortex tripole. These phenomena can also occur in real vortex configurations of fluids. *Conclusion.* Non-trivial scenarios for the transport of passive particles by a vortex tripole, which can also occur in real vortex configurations of fluids, have been discovered and described.

Keywords: vortex flows, system of point vortices, particle transfer, chaotic mixing, nonlinear systems, chaos.

Acknowledgements. This work was supported by Russian Foundation for Basic Research, grant No. 19-29-06013.

For citation: Govorukhin VN. Transfer of passive particles in the velocity field of vortex tripole moving on a plane. Izvestiya VUZ. Applied Nonlinear Dynamics. 2023;31(3):286–304. DOI: 10.18500/0869-6632-003039

Introduction

Multipole vortex configurations close to two-dimensional ones occur in nature and are reproduced in physical experiments [1–5]. A multipole is a configuration consisting of a central vortex and several satellites, with the center and satellites having a circulation (intensity) of opposite signs. Various mathematical models [6–8] are used to describe such structures, but the simplest is a system of point vortices. If we consider infinitely thin vortex filaments, and assume [9] that vorticity If it is focused on rectilinear threads parallel to each other, then we can consider the movement of the points of intersection of vortices with the plane. The image of such a vortex on a plane is a point, it is called a point vortex [10], which is described by coordinates on the plane and the value of circulation in it. Systems of even a small number of point vortices generate complex flows, and in many cases describe real hydrodynamic flows well. Thus, a similar mathematical model found application in the analysis of the instability of the vortex wake by von Karman in 1912, in the occurrence of large coherent vortices and in many other problems. Mathematically, the configuration of N point vortices is a Hamiltonian system of $2N$ ordinary differential equations. The study of such systems began, apparently, by Helmholtz [11] and is actively continuing to this day.

The simplest configuration on the plane, demonstrating a wide variety of motion modes depending on the parameters (intensity and mutual arrangement of vortices), is a system of three vortices, which explains the high interest in its study (see works [2, 12–16] and links in them). It is known that despite the integrability of the problem of dynamics of three vortices [17, 18] (due to the existence of a sufficient number of integrals), such configurations generate complex flows and non-trivial transfer processes in liquids. A special case of a three-vortex configuration is a point tripole, which consists of a central vortex located on the same straight line and two satellites located on opposite sides of it. The stability of the tripole, its dynamics, the structure of the velocity field generated by it are investigated, special attention is paid to the case of zero total circulation of the configuration (see [6,19,20] and references therein). The article [19] shows a good coincidence of the dynamics of liquid particles in the velocity field of a point tripole with the results of physical experiments.

The vortex configuration generates a velocity field that determines the mass transfer in the flow region. Liquid particles are called passive, which do not affect the movement of other particles, but are carried by the velocity field, and can demonstrate complex dynamics [21, 22]. Along with mathematical modeling of passive particle transport, other formulations of advection problems in a liquid are possible, which take into account various factors [23, 24], but such problems are not considered further in the work. The study of the processes of transport and mixing of passive particles can provide information about the processes occurring in the atmosphere, ocean, important for applications such as analysis of water currents, pollution transport, movement of cyclones and anticyclones [25, 26]. In particular, it is known that the velocity field of the configuration of three vortices in many cases generates chaotic transfer processes that demonstrate a variety of properties and non-trivial effects [14, 15, 19], which have not yet been fully studied.

The transfer of a passive particle by N point vortices can be interpreted as the dynamics of a system of $N+1$ vortices, and the intensity of the $(N+1)$ th vortex is zero. Mathematically, such a model is a system of ordinary differential equations, where the variables are the coordinates of vortices and passive particles, and the parameters are the intensity and location of vortices. Systems of ordinary differential equations are a classical tool for mathematical modeling of Lagrangian fluid dynamics. For their analysis, research methods based on the provisions of the theory of dynamical systems are effective (see, for example, [27–31]). These approaches include the search and analysis of invariant objects, their bifurcations, methods for studying chaotic

dynamics using Lyapunov exponents, Poincaré maps, etc. [32–36].

This article considers a vortex point tripole with zero total intensity, consisting of a central vortex (its intensity 2ω) and two satellites (with intensities −ω). The configuration in question can rotate in place (in the symmetric case), or it can move along the plane with rotation (if symmetry is broken). Despite its simplicity, such a mathematical model of vortex dynamics makes it possible to study many real processes and effects, to assess the influence of various disturbances and external influences on them. The main attention is paid to the study of the dynamics of passive particles and transport depending on their initial position at various parameters of the tripole that determine the speed of movement of the configuration. Due to the significant nonlinearity, most of the solved problems are amenable only to numerical analysis, which is the main research tool in the article. Due to the conservativeness of the system, when solving emerging Cauchy problems, methods of integration of a high order of accuracy are used in the work, which is necessary to preserve the integrals of the system. For a qualitative analysis of the dynamics and transport of particles, the construction of Poincare sections and the analysis of the dynamics of «marker segments» are used.

1. The simplest mathematical model of a vortex tripole

It is shown by Kirchhoff [9, 37] that the motions of N point vortices on the plane are described by the following Hamiltonian system of ordinary differential equations:

$$\omega_i \dot{x}_i = \frac{\partial H}{\partial y_i}, \quad \omega_i \dot{y}_i = -\frac{\partial H}{\partial x_i}, \quad H = -\frac{1}{4\pi} \sum_{i,j=1,\, i\neq j}^{N} \omega_i \omega_j \ln(r_{ij}) \quad i = 1 \ldots N. \tag{1}$$

Here (x_i, y_i) — coordinates of the vortex with the number i on the plane, $r_{ij} = (x_i - x_j)^2 + (y_i - y_j)^2$, and ω_i — its intensity (circulation). It is obvious that H is the Hamiltonian and the first integral of the system (1). The intensity of vortices and their initial coordinates can be considered as parameters of the system. The initial values determine the values of the integrals of the point vortex system, which means that the invariant subspaces on which the dynamics occurs. The current function for a passive particle in the velocity field of a system of point vortices has the form

$$\Psi = -\frac{1}{4\pi} \sum_{i=1}^{N} \omega_i \ln[(x - x_i)^2 + (y - y_i)^2], \tag{2}$$

where (x, y) are the coordinates of the passive particle on the plane. That is , the dynamics of a particle is described by a system of two ordinary differential equations

$$\dot{x} = \frac{\partial \Psi}{\partial x} = -\sum_{i=1}^{N} \frac{\omega_i}{2\pi} \frac{y - y_i}{(x - x_i)^2 + (y - y_i)^2}, \quad \dot{y} = -\frac{\partial \Psi}{\partial y} = \sum_{i=1}^{N} \frac{\omega_i}{2\pi} \frac{x - x_i}{(x - x_i)^2 + (y - y_i)^2}. \tag{3}$$

From (3) it can be seen that the effect on a passive particle of a system of vortices is equal to the sum of the effects of all vortices on it, and at an infinitesimal moment of time each vortex spins the particle in a circle around itself at a speed directly proportional to the intensity and inversely proportional to the square of the distance between the vortex and the particle.

In addition to the Hamiltonian, the system (1), by virtue of invariance with respect to transfer and rotation, has three more first integrals:

$$Q = \sum_{i=1}^{N} \omega_i x_i, \quad P = \sum_{i=1}^{N} \omega_i y_i, \quad I = \sum_{i=1}^{N} \omega_i (x_i^2 + y_i^2). \tag{4}$$

The integral H expresses the law of conservation of the energy of interaction of vortices, and the integrals (4) are analogs of the laws of conservation of momentum components and angular momentum for point vortices. Consequently, the dynamics of a system of N vortices for $N = 2, 3$ is integrable, but for $N \geqslant 4$ this is no longer the case, and its behavior may be chaotic. The nonintegrability of the system of four vortices is strictly proved in [38]. Note that for $N = 2, 3$, while the system itself (1) is integrable, the behavior of a passive particle, that is, the system (1)–(3) may exhibit chaotic dynamics.

Next, a tripole is considered, which consists of a central point vortex C and its two satellites S_1 and S_2, and the intensities of the satellites have opposite signs with the center. The interest in analyzing the movements of vortex dipoles is due to the fact that they are observed in nature and implemented in physical experiments [1]. Such configurations may have a small total circulation, and two satellites — similar intensities [2]. We will consider the idealization of such a structure: it is assumed that the central vortex C has the intensity $\omega_1 = 2\omega$, and each of the satellites $\omega_2 = \omega_3 = -\omega$. We assume that at the initial moment of time S_1 is located on the plane at a point with coordinates $x = 0$, $y = -d$, S_2 — at $x = 0$, $y = d$, and C — at the point $x = 0$, $y = \varepsilon$.

Then the system of equations describing the dynamics of the vortex three fields and passive particles will take the following form in coordinate form:

$$\begin{cases} \dot{x}_1 = -\dfrac{\omega}{2\pi}\left(\dfrac{y_1 - y_2}{r_{12}} + \dfrac{y_1 - y_3}{r_{13}}\right), & \dot{y}_1 = \dfrac{\omega}{2\pi}\left(\dfrac{x_1 - x_2}{r_{12}} + \dfrac{x_1 - x_3}{r_{13}}\right), \\ \dot{x}_2 = -\dfrac{\omega}{2\pi}\left(\dfrac{-2(y_1 - y_2)}{r_{21}} + \dfrac{y_2 - y_3}{r_{23}}\right), & \dot{y}_2 = \dfrac{\omega}{2\pi}\left(\dfrac{-2(x_1 - x_2)}{r_{21}} + \dfrac{x_2 - x_3}{r_{23}}\right), \\ \dot{x}_3 = -\dfrac{\omega}{2\pi}\left(\dfrac{-2(y_1 - y_3)}{r_{31}} + \dfrac{y_3 - y_2}{r_{32}}\right), & \dot{y}_3 = \dfrac{\omega}{2\pi}\left(\dfrac{-2(x_1 - x_3)}{r_{31}} + \dfrac{x_3 - x_2}{r_{32}}\right), \\ \dot{x} = -\dfrac{\omega}{2\pi}\left(\dfrac{2(y - y_1)}{(x_1 - x)^2 + (y_1 - y)^2} + \dfrac{y - y_2}{(x_2 - x)^2 + (y_2 - y)^2} + \dfrac{y - y_3}{(x_3 - x)^2 + (y_3 - y)^2}\right), \\ \dot{y} = \dfrac{\omega}{2\pi}\left(\dfrac{2(x - x_1)}{(x_1 - x)^2 + (y_1 - y)^2} + \dfrac{x - x_2}{(x_2 - x)^2 + (y_2 - y)^2} + \dfrac{x - x_3}{(x_3 - x)^2 + (y_3 - y)^2}\right), \end{cases} \tag{5}$$

where (x_1, y_1) — coordinates of the vortex C, (x_2, y_2), (x_3, y_3) — coordinates of S_1 and S_2, respectively, and (x, y) — coordinates of the transferred particle. The studied point vortex tripole is determined by the following initial conditions:

$$x_1(0) = 0, \quad y_1(0) = \varepsilon, \quad x_2(0) = 0, \quad y_2(0) = -d, \quad x_3(0) = 0, \quad y_3(0) = d. \tag{6}$$

Next, the calculations take $\omega = 1$, $d = 1$. Note that ω and d can always be taken equal to one due to the choice of time scales and spatial coordinates. Thus, in the problem under consideration (5), (6) only one parameter ε will remain, which determines the configuration asymmetry.

The dynamics of a system of three point vortices with zero total intensity is well studied (see [12, 19, 20, 39–41] and references therein). In the article [19] , a special case of the system of equations (5) is also considered in detail. In particular, a good coincidence of the dynamics of the mathematical model with physical experimental observations is shown. Following this work, we present the facts necessary for studying the transfer of a passive particle about the dynamics of a point vortex tripole with a change in the parameter ε.

For an unperturbed ($\varepsilon = 0$) symmetric tripole, both components of the momentum are $P = Q = 0$, and $I = -2\omega \neq 0$. This means that the central vortex remains in place, and the satellites rotate around C counterclockwise. When $\varepsilon = 0$, an expression is known for the rotation

period $T_0 = 2\pi d^2/(3\ omega)$. When $0 < \varepsilon < \varepsilon_c$, the structure loses symmetry, but retains a tripolar topology, $P = 2\omega\varepsilon \neq 0$ and $I = -2\omega(1-\varepsilon^2) \neq 0$. Both satellites S_1 and S_2 rotate around the central vortex C in a positive direction, and the entire configuration moves on a plane along the horizontal coordinate axis with an average velocity for the period T $\langle v_x \rangle$. The direction of movement is determined by the sign ε, with $\varepsilon > 0$ — movement to the right. At the same time, in the mobile coordinate system $x' = x - x_1$, $y' = y - y_1$, where the point $(0,0)$ corresponds to the position of the center of the tripole C, the dynamics of the tripole is periodic with the period $T = T(\varepsilon)$. During the time $0 < t < T$, the distances $d_1 = \|C - S_1\|$ and $d_2 = \|C - S_2\|$ and the angle between the segments $[C, S_1]$ and $[C, S_2]$ change, but at $t = k\,T$, $k = 1, 2, \ldots$ the tripole returns to its original position in the moving coordinate system. In coordinates (x, y) for $t = k\,T$, the vortex C has coordinates $(kT\ \langle v_x \rangle, \varepsilon)$, and S_1 and S_2 respectively $(kT\ \langle v_x \rangle, -d)$ and $(kT\ \langle v_x \rangle, d)$. At $\varepsilon > \varepsilon_c$ (with the parameter values selected for numerical analysis, the critical value of $\varepsilon_c \approx 0.544$), the vortex configuration switches from a tripole to a dipole-monopole mode when the vortex C and one of the satellites form a moving dipole. This case is not considered in this paper.

The dynamics of a vortex point tripole on the plane (x, y) is illustrated in Fig. 1, *a*, which shows the trajectories of the center C, satellites S_1 and S_2 with $\varepsilon = 0.4$ by $t \in [0, 6T]$. In addition, the positions of the tripole are shown for three time points t ($t = 10.16 \approx 6T$ corresponds to six turns of the tripole), where the circle indicates the position of the center C, the square — of the satellite S_1 and the rhombus — S_2. In Fig. 1, *b* graphs of the periodic dependence of the distances d_1 and d_2 on time for $t \in [0, 4T]$ are given. In addition, Fig. 1, *a* demonstrates the movement of the tripole to the right along the x axis with some speed $\langle v_x \rangle$. The value of $\langle v_x \rangle$ depends on the parameter ε and was constructed numerically (Fig. 1, *c*). When $\varepsilon < 0.2$ the average velocity

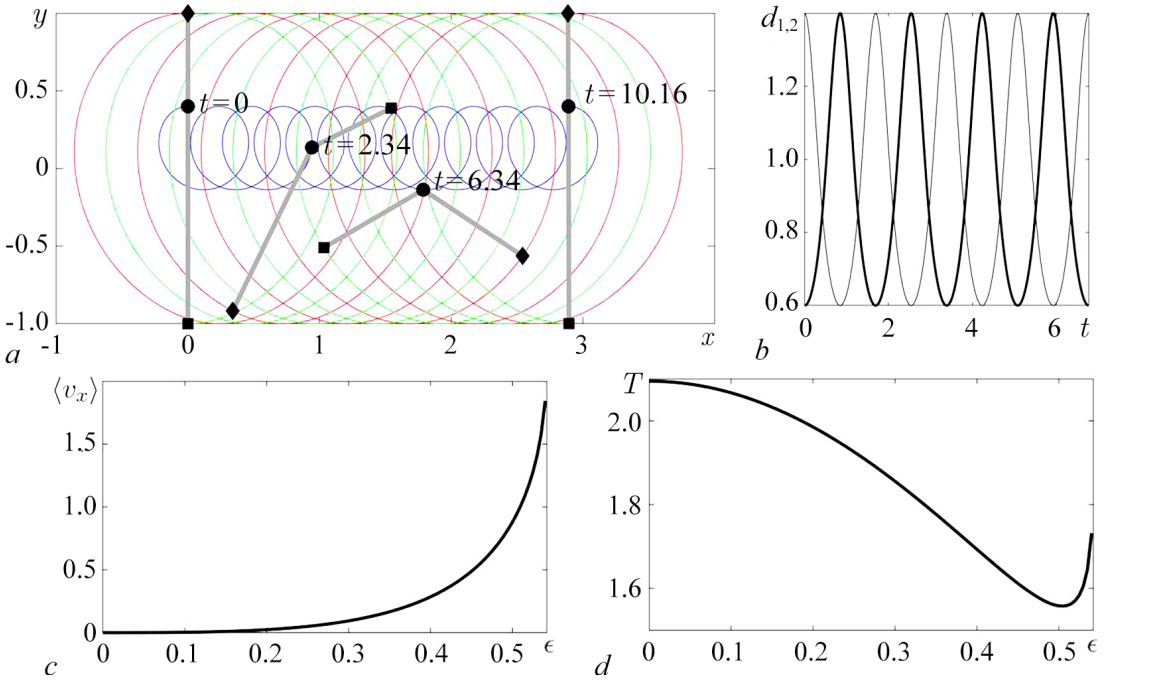

Fig. 1. *a* — Tripole dynamics at $\varepsilon = 0.4$. The trajectory of the center C (blue curve, circled) and satellites S_1 (green, square) and S_2 (red, rhombus) are shown. *b* — Graphs of the periodic dependence of the distances d_1 (thin line) and d_2 (thick line) on $t \in [0, 4T]$. *c* — Graph of the dependence of the tripole velocity $\langle v_x \rangle$ averaged over the period T on the ε parameter. *d* — Graph of the dependence of the period of rotation of the satellites of the tripole around its center on the parameter ε (color online)

of the tripole moving along the plane is small, $\langle v_x \rangle < 0.1$, but at $\varepsilon > 0.2$ there is a significant increase in it, and $\langle v_x \rangle$ at $\varepsilon \approx \varepsilon_c$ almost reaches the value of 2.0. The period of the complete turnover of the tripole also depends on the parameter ε (Fig. 1, *d*).

The purpose of the study presented here is to study how the parameter ε, and hence the magnitude of the displacement velocity of the tripole $\langle v_x \rangle$ on the plane, affects the transport properties of passive particles. In the works cited above [19, 20, 41], the study of the influence of the parameter ε was considered, but the study of, basically, it was carried out in a movable (centered in C) coordinate system $x' = x - x_1$, $y' = y - y_1$. In this case, the dynamical system for the tripole and passive particles (5) can be reduced to a canonical form, and considered from the standpoint of KAM theory (see the provisions of the theory in [42, 43] and in the references to the literature in these works). It is possible to prove the integrability of the system at $\varepsilon = 0$, to find singular points, to obtain an expression for the Melnikov function [19], which allows us to evaluate the occurrence and development of chaotic regions. However, the author failed to study the dependence of the properties of particle transport by a tripole on the velocity $\langle v_x \rangle$ on the plane (x, y) in previous works.

2. Analysis of particle dynamics in the velocity field three fields

From the equations of transport of passive particles in the velocity field of point vortices (5) it follows that $|\dot{x}| \to 0$ and $|\dot{y}| \to 0$ for $r(x, y) \to +\infty$, where $r(x, y)$ is the distance from the particle to C. This means that there is practically no movement of passive particles far from the tripole, and active mixing and transfer of particles occur in the vicinity of the vortex configuration. Additional studies are required to study the size and shape of the mixing area, the nature of particle dynamics and other processes accompanying the movement of the tripole. Due to the nonlinearity of the emerging problems, analytical methods for solving them fail, and the use of numerical approaches is required.

In the study of passive particle transport in this paper, most calculations were carried out at intervals of $t \in [0.1000T]$ and more. Such longtime calculations place high demands on the choice of methods for solving the Cauchy problem and constructing the Poincare mapping, especially for systems with the first integrals. Such tasks include the calculation of particle dynamics of an incompressible inviscid fluid (see the article [44] and references therein). It is known that all explicit integrators for systems of ordinary differential equations do not preserve nonlinear integrals (the magnitude of these violations is determined by the order of the method), which can lead to qualitatively incorrect numerical results. A possible way to minimize this problem over long periods is to use special geometric integrators [45], for example, symplectic methods lead to fluctuations in the calculated values of integrals in the vicinity of true values. However, such methods are implicit, which creates difficulties in their implementation and increases computational costs, especially for high orders of accuracy. An alternative is the «power» approach — the use of explicit methods of high-order accuracy with a small integration step, which is used in the presented article. This approach allows you to maintain a small error in the values of integrals over long calculation times.

The work used Runge-Kutta methods of 7, 8 and 9 orders of accuracy with automatic step selection and accuracy control using «nested formulas», see [46]. All calculations and visualization of the results were carried out in the environment of the MATLAB package using the built-in functions for solving the Cauchy problem ode78 (method order 7/8) and ode89 (method order 8/9) (for a description of the methods, see [47]). In addition, the Runge–Kutta Dorman–Prince method of 7/8 order of accuracy [48] and its software implementation ode87 [49] were used. This method was the main one in the numerical study and calculation of Poincare mapping points. The

calculations used the relative error rel $= 10^{-10}$, the maximum step $h_{\max} = 0.05$, the condition of belonging to the secant Poincare $|x_1 - x_2| < 10\,\mathrm{rel}$). The step was limited in order to reduce the influence of the integration step control algorithm. To clarify the trajectory point on the secant, the Newton method was used. This approach ensured the preservation of the invariants of the problem with the necessary high accuracy. In all the calculations performed, the integrals P and Q, see (4), were preserved exactly, and the error in calculating I and H, see (1), did not exceed 10^{-8} in the interval $t \in [0.1000T]$. To check the correctness of the calculations, the calculations were repeated with rel $= 10^{-11}$ and using the integrators ode78 and ode89. All numerical results were reproduced.

2.1. Dynamics of passive particles in a moving coordinate system (x', y')**.** Let's study the changes in the dynamics of the system (5) on the plane (x', y') when changing ε. In Fig. 2 on the plane (x', y'), calculated Poincare mapping points are given for various 32 trajectories and six values of ε. The Poincare secant is given by the condition $x_1 - x_2 = 0$, $y_2 < 0$, which corresponds to the total turnover of the tripole (one period T) with the given parameters. 3,500 intersections are calculated for each trajectory (that is, $t \in [0, 3500\,T]$). The starting points of the trajectories are identical for all ε.

When ε $= 0$, the system is integrable, $x = x'$, $y = y'$, the entire vortex configuration rotates around the center of C, which is at the point $x = 0$, $y = 0$ for all t. On the Poincare plane, three fields correspond to elliptical singular points and there are two saddle fields connected by separatrices (see Fig. 2). At initial values from the Poincare plane, quasi-periodic motions are realized in zones not separated by separatrices, including elliptical singular points. They

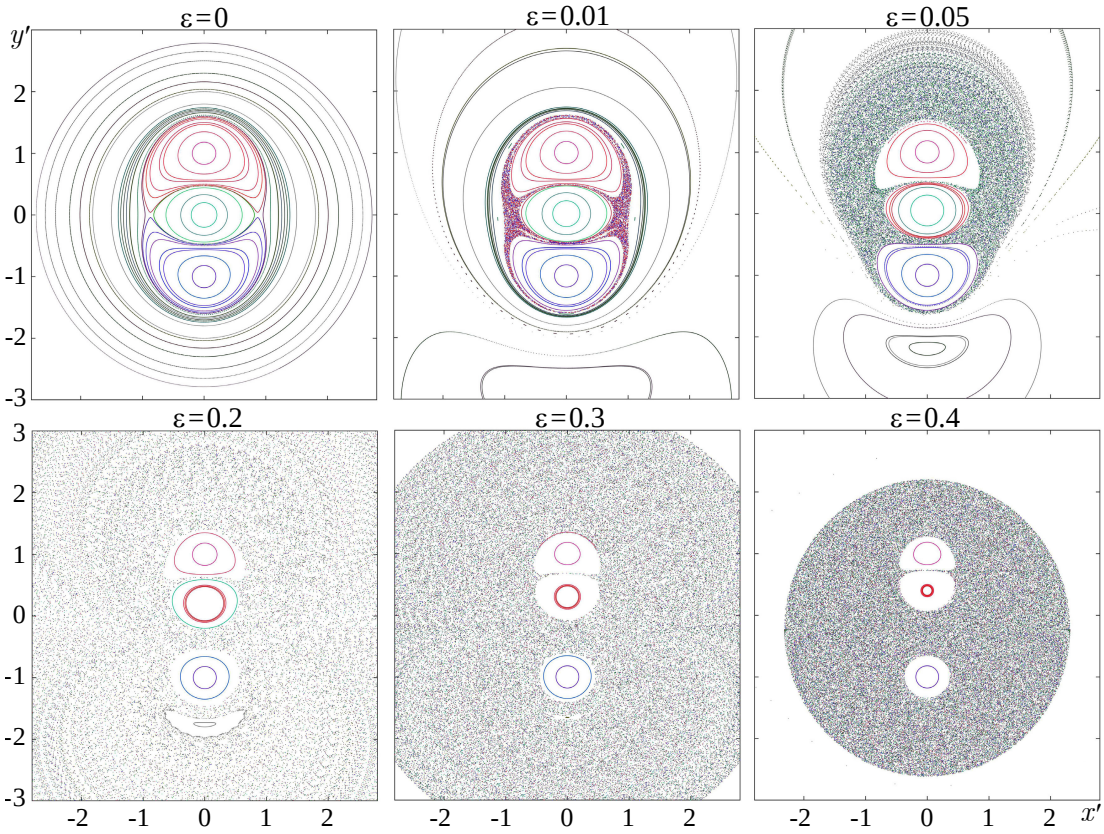

Fig. 2. Poincaré map by the section $x_1 - x_2 = 0$, $y_2 < 0$ on the plane (x', y') for different values of ε, calculated 32 trajectories, each marked with its own color (color online)

correspond to closed curves in the Poincare mapping, and all of them cover a vortex tripole at $\varepsilon = 0$.

At $\varepsilon \neq 0$ integrability and symmetry of the dynamical system (5) is violated, according to KAM theory, regions of chaotic dynamics arise in the vicinity of separatries. For small perturbations, see the case $\varepsilon = 0.01$, the width of the chaotic region is small. In addition, the topological structure of the Poincare mapping changes qualitatively in the variables (x', y') and beyond the chaos domain. An additional elliptical singular point of multiplicity 1 arises outside the region of the vortex three field. Quasi-periodic motions around this singular point do not cover the tripole, see the lower part of Fig. 2, $\varepsilon = 0.01$. That is, two qualitatively different regions are formed on the Poincare plane, which are separated by a separatrix.

With the growth of ε, the size of the chaotic region increases, shifts to the half-plane $y' > 0$. The intensity of particle mixing depends on the position in the chaotic region, is stronger in the vicinity of the tripole vortices, and decreases as it approaches the boundary of the chaotic region. Near the boundaries of the chaotic region, the particle motions are close to quasi-periodic by (x', y') with a small radial displacement with respect to the tripole. These effects are demonstrated by Fig. 2, $\varepsilon = 0.05$. Increasing ε leads to the development of a chaotic region, which has a maximum size at $\varepsilon \approx 0.2$. The growth of the perturbation at $\varepsilon > 0.2$ is accompanied by an increase in the velocity of the tripole $\langle v_x \rangle$ (see Fig. 1, *c*), reducing the size of a single chaotic region (see fig. 2, $\varepsilon = 0.3$), which takes the form of a circle with small zones of regular dynamics in the vicinity of the tripole vortices (see Fig. 2, $\varepsilon = 0.4$). All trajectories with initial data outside the chaos zone at $\varepsilon > 0.3$ are rapidly shifting in the direction of $x' \to -\infty$.

2.2. Dynamics of passive particles on the plane (x, y). To analyze the transfer of particles by a moving tripole in the initial coordinates (x, y), consider the change of «marker segments» on the plane in time. The marker segment $l(x_0, t, b, n)$ means a set of n passive particles with the same initial coordinate $x^{(i)} = x_0$ and coordinates $y^{(i)} = -b + i\, h_y$, $i = 0, \ldots, n$, $h_y = 2b/n$. Tracking the transformation of marker segments with the growth of perturbation in time allows us to study the transfer of passive particles in the velocity field of the vortex configuration. In numerical experiments, the value $T = T(\varepsilon)$ was used as a characteristic time, corresponding to the total rotation of the satellites around the center of the tripole, which depends on the magnitude of the disturbance. Also, the speed of the $\langle v_x \rangle$ of the tripole movement along the plane (x, y) depends on ε, see the previous section and Fig. 1. In the calculations presented below, four marker segments $l(x_0, t, b, k)$ were used for $x_0 = -5, -2, 2, 5$ with $b = 6$, $k = 1000$. That is, in each calculation, the Cauchy problem was solved for a system of equations (5) consisting of 6 equations describing the dynamics of point vortices and $n = 1000 \times 4 \times 2 = 8000$ equations for particles specifying $l(x_0, t, 6, 1000)$, $x_0 = -5, -2, 2, 5$. The results are presented graphically, the initial positions of the marker segments for all calculations are illustrated in Fig. 3. In the figures, the particles of each marker segment are marked with the same color and symbol.

In the symmetric case ($\varepsilon = 0$), the vortices S_1 and S_2 rotate around the center of C at a constant speed, the tripole does not move along the plane, $\langle v_x \rangle = 0$. Then $x = x', y = y'$ and the structure of the passive particle current lines on the plane (x, y) is described in Fig. 2. In this case, the transfer of particles is regular with high velocity in the vicinity of the vortex configuration, and attenuates when moving away from it. This is illustrated by the dynamics of marker segments shown in Fig. 3. Deleted segments $l(-5, t, 6, 1000)$ and $l(5, t, 6, 1000)$ are practically not affected by the tripole at times of the order of hundreds of revolutions, and only at times of the order of $1000\,T$ and above, their slight deformation is observed. For segments $l(-2, t, 6, 1000)$ and $l(2, t, 6, 1000)$ the situation is different — their middles fall into the area of rapid movements in the vicinity of the tripole, stretch and transform, the particles belonging to them rotate around the tripole. The ends of the marker segments practically do not change their

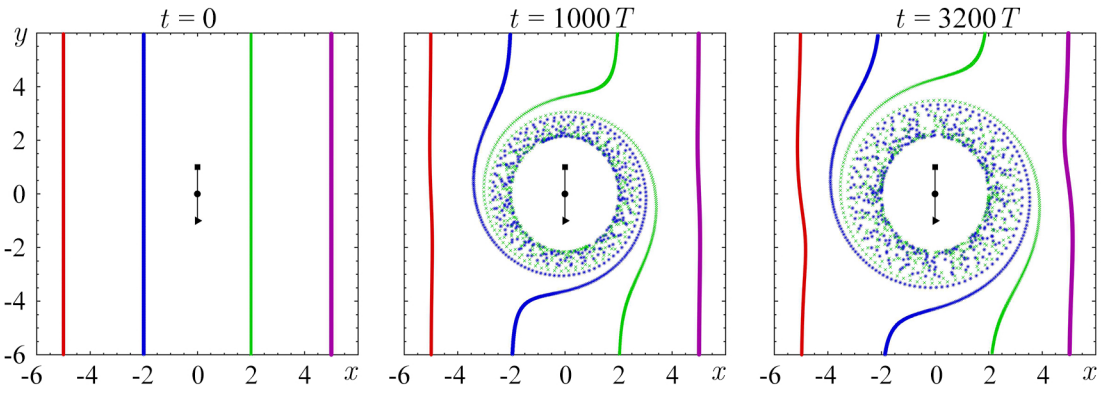

Fig. 3. Marker segments on the plane (x, y) at the initial time $t = 0$, and for $t = 1000\,T$, $3200\,T$, i.e. after 1000 and 3200 full rotations of the tripole at $\varepsilon = 0$. Symbols connected by lines depict a vortex tripole (color online)

position, since they are located in areas with low speed $\dot{x}^{(i)}$, $\dot{y}^{(i)}$.

At $\varepsilon > 0$, the symmetry of the tripole is broken, the vortex configuration moves at a speed of $\langle v_x \rangle$ along the abscissa axis on the plane (x, y), the structure of the phase space of the dynamical system for passive particles (5) in coordinates changes qualitatively (x', y'), see the previous subsection and Fig. 2. The changes in the transfer processes with the growth of ε are well illustrated by the transformations of marker segments. For small $\varepsilon > 0$ $\langle v_x \rangle \ll 1$, the movement of the tripole is slow, but the transfer structure is fundamentally different from the symmetric case of $\varepsilon = 0$. In Fig. 4 the calculation results are given for $\varepsilon = 0.05$ when $\langle v_x \rangle = 0.0003$, $T = 2.0874$. It can be seen that between the tripole and the resulting stagnant zone (with the center coordinate $y \approx -2$) there is a region of rapid movement of particles from the area to

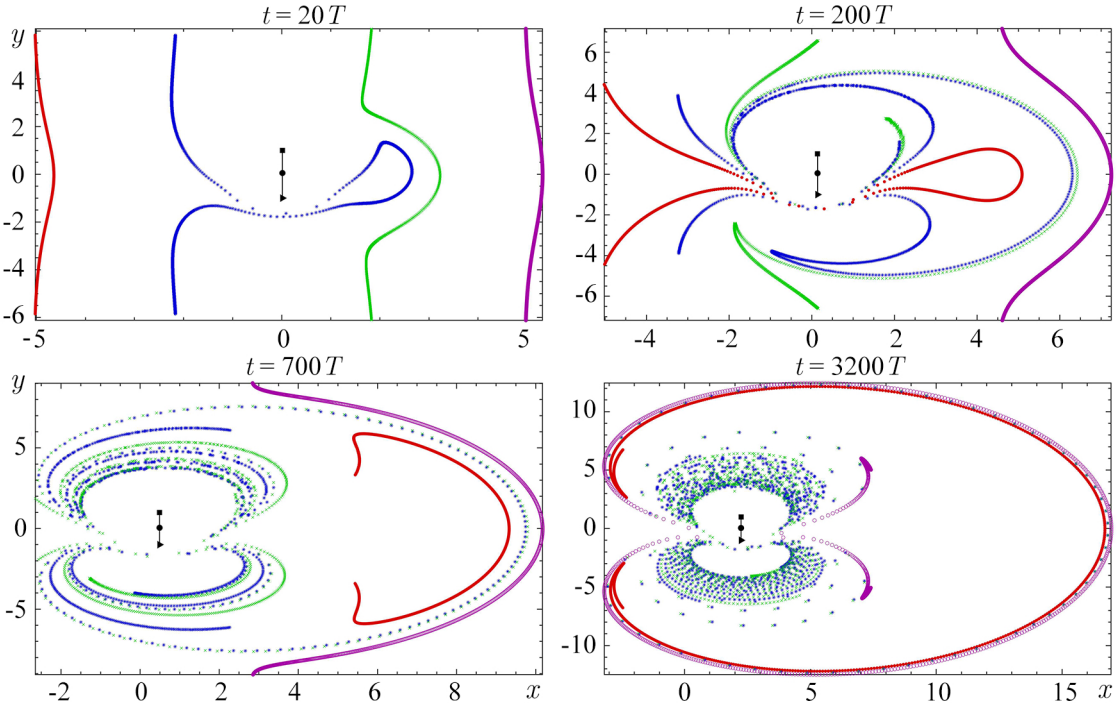

Fig. 4. The position of particles of marker segments $l(x_0, t, 6, 1000)$ for $x_0 = -5, -2, 2, 5$ at $\varepsilon = 0.05$ at different times (color online)

the left of the tripole to the right (see Fig. 4, $t = 20\,T$, $200T$). At long times corresponding to hundreds of revolutions of the tripole, both marker segments with $x_0 < 0$ completely move to the right of the tripole ($t = 700\,T$).Some of the particles of segments with $x_0 > 0$ (with the y coordinate at the vortex level) stretch and shift along the motion of the vortex configuration, and the rest — against the motion (see Fig. 4, $t = 10\,T, 350\,T$). At long times (more than several thousand revolutions of the tripole), these particles fall into the half-plane $x < x_1(t)$, slowly tend to the region of particle overflow, and are transferred through the region of rapid movement into the half-plane $x > x_1(t)$. Note that the dynamics of each particle of the marker segments is not regular (that is, they all fall into the area of chaotic dynamics) and consists of slow and fast movements. Slow ones consist in close to quasi-periodic movements far from the tripole, and at the same time the distance to the tripole can both increase and decrease. Fast movements occur in the vicinity of point vortices, and consist in their transfer from the region $x < x_1(t)$ in $x > x_1(t)$ or in chaotic movements near tripole vortices. This is illustrated by the trajectory of one of the particles constructed for $t \in [0,\ 25000\,T]$, and shown in Fig. 5. It can be seen that it consists of qualitatively different sections. So, curves marked with the symbols $1, 2, 5$ correspond to slow irregular dynamics, and $3, 4$ — chaotic movements in the vicinity of the tripole. Thus, at $\varepsilon = 0.05$, a vast area of chaotic dynamics arises, and it consists of two qualitatively different subdomains - active and slow mixing. The area of chaotic dynamics on the plane (x', y') is given in Fig. 2, $\varepsilon = 0.05$.

An increase in ε leads to a growth in the zone of chaotic dynamics and an expansion of the subdomain of active mixing of particles. These processes can be seen in Fig. 6 where the positions of the marker segment particles are given for different values of T and $\varepsilon = 0.1$. With this parameter value, the speed of the tripole movement is an order of magnitude greater than with $\varepsilon = 0.05$, but remains small $\langle v_x \rangle = 0.0027$, the time of the complete tripole revolution $T = 2.0667$. And in this case, the marker segments with $x_0 < 0$ completely pass into the area of $x > x_1(t)$ after approximately 500 revolutions of the tripole, but at the same time the particles immediately fall into the region of strong mixing in the vicinity of the tripole, see $t = 20\,T$, $200\,T$.

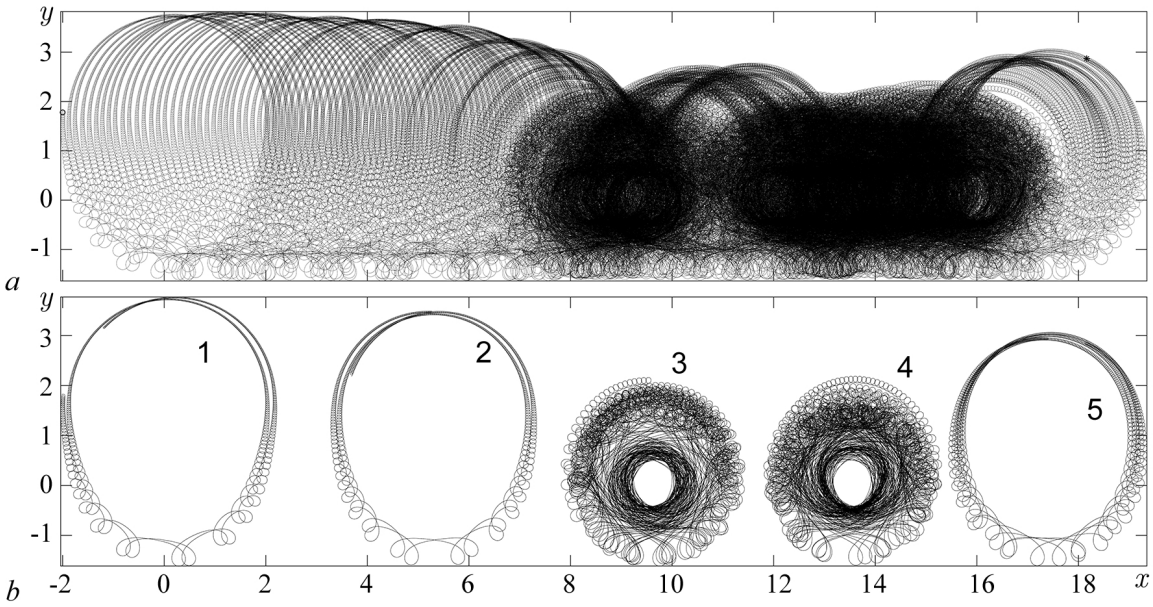

Fig. 5. Trajectory of one of the passive particles on the (x, y) plane at $\varepsilon = 0.05$. a — Over the entire time interval $t \in [0,\ 25000\,T]$; b — five sections of the trajectory for: 1 — $t \in [0, 350\,T]$, 2 — $t \in [7450\,T, 7800\,T]$, 3 — $t \in [13500\,T, 13850\,T]$, 4 — $t \in [19200\,T, 19550\,T]$, 5 — $t \in [24650\,T, 25000\,T]$

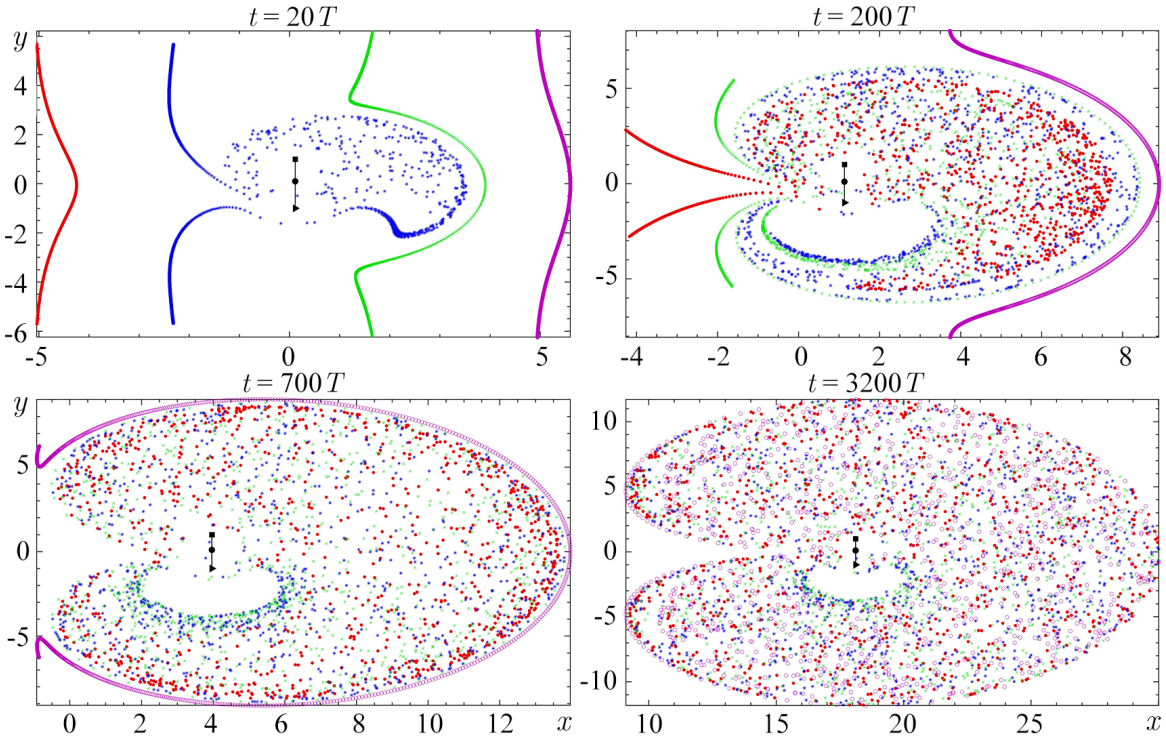

Fig. 6. The position of the particles of the four marker segments at ε = 0.1 at different times (color online)

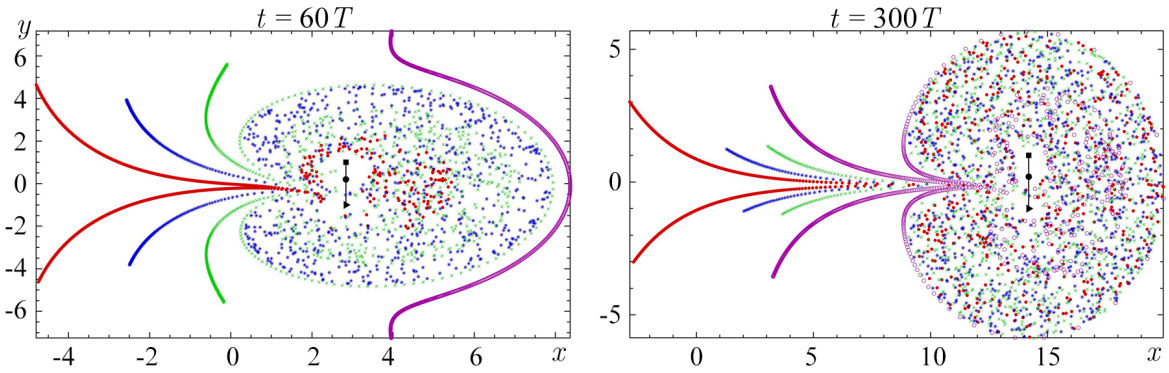

Fig. 7. The position of the particles of the four marker segments at ε = 0.2 at different times (color online)

At $t = 3200\,T$, the particles of all four marker segments are mixed together and are in the region of chaotic dynamics. That is, with such a tripole geometry, the entire vortex structure moves at low speed along the x axis, dragging particles from a wide area around it into the region of strong mixing. In addition, all the particles of the marker segments are transferred to a sufficiently large distance together with the tripole (see Fig. 6, $t = 3200\,T$).

Further growth of the symmetry disturbance of the three fields leads to a qualitative change in the structure of the transfer of marker segments. In Fig. 7 the results of calculations for ε=0.2 are given. With this parameter value, the speed of movement $\langle v_x \rangle = 0.0238$, that is, it has increased by almost an order of magnitude, and the period has decreased, $T = 1.985$. The fundamental change in the transfer of particles is that at such a speed $\langle v_x \rangle$ not all the particles of the marker segments fall into the vicinity of the tripole, and remain in the region $x < x_1(t)$, since

the speed of their movement is less than $\langle v_x \rangle$, and decreases with the growth of t. The remaining particles fall into the area of chaos, as in the previous cases. The zone of chaotic dynamics shifts along with the vortex configuration, particles of all four marker segments are present in it.

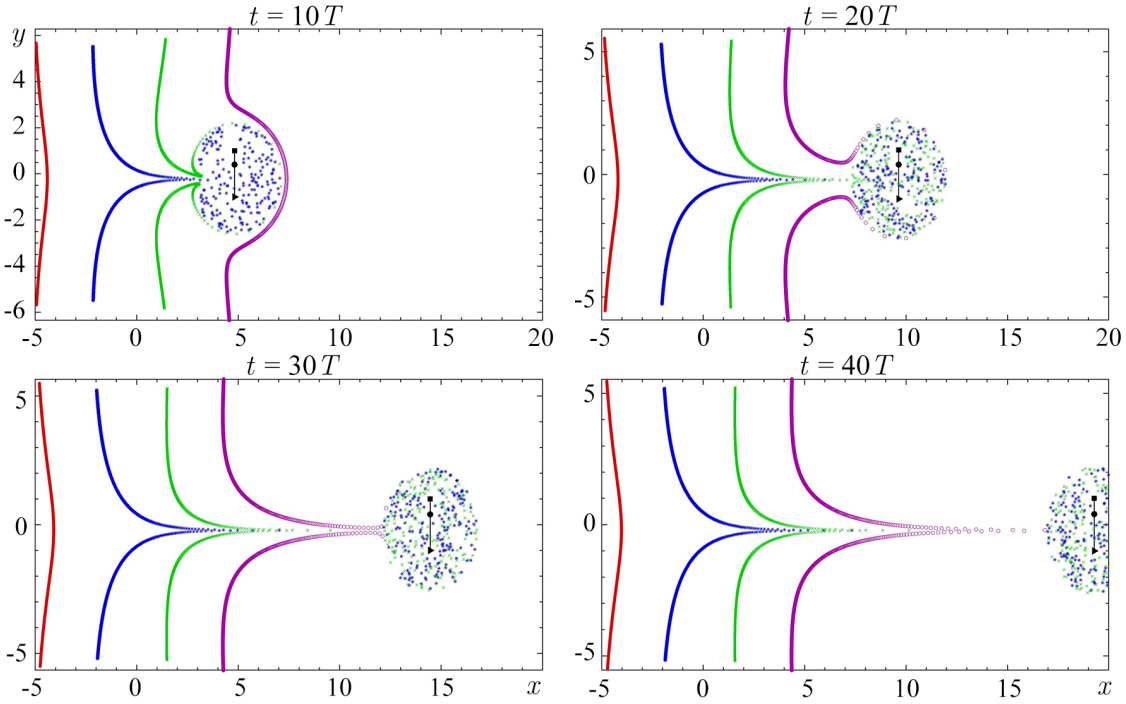

Fig. 8. The position of the particles of the four marker segments at $\varepsilon = 0.4$ at different times (color online)

The subsequent increase in ε leads to a significant increase in the velocity of the $\langle v_x \rangle$ movement of the vortex configuration (see Fig. 1, *c*), the acceleration of rotation (see fig. 1, *d*), and reducing the chaos area on the plane (x', y') (see fig. 2 with $\varepsilon = 0.3,\ 0.4$). This radically changes the dynamics of passive particles and their transfer to the velocity field of the tripole. In Fig. 8 in the same coordinate axes on the plane (x, y), the positions of the marker segment particles at four time points are given at $\varepsilon = 0.4$ ($\langle v_x \rangle = 0.2846$, $T = 1.6931$). In this case, the tripole captures part of the particles of the marker segments $l(-2, t, 6, 1000)$ and $l(2, t, 6, 1000)$, and they fall into the realm of chaos. The remaining particles of these segments shift at the first stage of dynamics, and with the removal of the tripole, their velocities tend to zero, and the particles stop. All marker particles are $l(-5, t, 6, 1000)$ remain close to the starting position. Segment $l(5, t, 6, 1000)$ at the first stage stretches, then the tripole «passes through» this marker segment, and with the removal of the tripole, most of its particles (and possibly all) stops. At all times $t \in [0,\ 1000T]$ considered in the numerical experiment, only particles of segments $l(-2, t, 6, 1000) are in the chaos region$ and $l(2, t, 6, 1000)$. This suggests that when moving at a sufficiently high speed, the vortex tripole carries particles from the vicinity of the initial position, and practically does not capture new particles along its path along the x axis, the particles ahead of its movement «flow around» a chaotic region.

Conclusion

The transfer of passive particles in the velocity field of a vortex tripole is studied in the article. To describe the vortex structure, the simplest classical mathematical model is used —

a system of point vortices. A tripole is a configuration consisting of a central vortex and two satellites, and the intensities of the center and the satellites are opposite in sign, all three vortices are located at the initial moment on the same straight line, the center is located between the satellites. In this paper, consideration is limited to the special case of a tripole with zero total intensity, when the intensity module of the center is twice as large as the intensity modules of each of the satellites. In the symmetric case (when the distances from the center to the satellites are the same at the initial moment), the center of such a configuration remains in place, and the satellites rotate around the center. When symmetry is broken (the distances between the satellites and the center are different), the entire configuration moves along the plane, and the greater the distance difference, the greater the speed of movement. The analysis of the influence of the magnitude of the symmetry perturbation of the tripole, and hence the velocity of its movement, on the processes of passive particle transfer is carried out.

Mathematically, the model is formulated as a system of nonlinear ordinary differential equations with the parameter — the magnitude of the tripole perturbation. The study was carried out numerically using high-order precision integrators and algorithms based on the approaches of the theory of dynamical systems, including the construction of the Poincare mapping and the analysis of the transformation of <marker segments>, which are a set of passive particles located on the segment at the initial moment. Calculations were carried out at long times corresponding to hundreds and thousands of revolutions of the three fields around its center.

As a result of numerical research, it was found that the transfer of passive particles is fundamentally different at low and high speeds of the tripole movement along the plane. When the velocity is small (with small tripole perturbations), a vast region of chaotic dynamics arises in the vicinity of the vortex configuration, which consists of two qualitatively different subdomains - active and slow mixing. The entire region slowly shifts along with the tripole, and the tripole acts as a «mixer», moving and mixing particles from the left area to the right, and this process captures a large area on the plane. At a sufficiently high velocity of the vortex tripole, the chaotic dynamics region is significantly smaller, it consists entirely of an active mixing region. In this case, the vortex configuration is a "carrier"that moves particles from the vicinity of its initial position over long distances, and practically does not capture new particles along its path. In intermediate situations, to varying degrees, which is determined by the perturbation parameter, both processes are implemented. It is natural to assume that real tripolar vortex configurations of liquids and gases can demonstrate similar dependences of the transfer properties on their geometry and velocity of movement.

References

1. van Heijst GJF, Kloosterziel RC. Tripolar vortices in a rotating fluid. Nature. 1989;338(6216): 569–571. DOI: 10.1038/338569a0.
2. Kloosterziel RC, van Heijst GJF. An experimental study of unstable barotropic vortices in a rotating fluid. J. Fluid Mech. 1991;223:1–24. DOI: 10.1017/S0022112091001301.
3. Carnevale GF, Kloosterziel RC. Emergence and evolution of triangular vortices. J. Fluid Mech. 1994;259:305–331. DOI: 10.1017/S0022112094000157.
4. Trieling RR, van Heijst GJF, Kizner Z. Laboratory experiments on multipolar vortices in a rotating fluid. Physics of Fluids. 2010;22(9):094104. DOI: 10.1063/1.3481797.
5. Rostami M, Zeitlin V. Evolution of double-eye wall hurricanes and emergence of complex tripolar end states in moist-convective rotating shallow water model. Physics of Fluids. 2022;34(6):066602. DOI: 10.1063/5.0096554.
6. Carton X, Legras B. The life-cycle of tripoles in two-dimensional incompressible flows. J. Fluid Mech. 1994;267:53–82. DOI: 10.1017/S0022112094001114.
7. Kizner Z, Khvoles R. The tripole vortex: Experimental evidence and explicit solutions.

Phys. Rev. E. 2004;70(1):016307. DOI: 10.1103/PhysRevE.70.016307.
8. Viúdez A. A stable tripole vortex model in two-dimensional Euler flows. J. Fluid Mech. 2019;878:R5. DOI: 10.1017/jfm.2019.730.
9. Kirchhoff G. Vorlesungen über mathematische Physik. Bd. 1: Mechanik. Leipzig: Teubner; 1876. 489 s. (in German).
10. Batchelor GK. An Introduction to Fluid Dynamics. 2nd edition. Cambridge: Cambridge University Press; 2000. 658 p. DOI: 10.1017/CBO9780511800955.
11. Helmholtz H. Über Integrale der hydrodynamischen Gleichungen, welche den Wirbelbewegungen entsprechen. Journal für die reine und angewandte Mathematik. 1858;55:25–55 (in German). DOI: 10.1515/crll.1858.55.25.
12. Aref H. Motion of three vortices. Physics of Fluids. 1979;22(3):393–400. DOI: 10.1063/1.862605.
13. Borisov AV, Mamaev IS, Vaskina AV. Stability of new relative equilibria of the system of three point vortices in a circular domain. Russian Journal of Nonlinear Dynamics. 2011;7(1):119–138 (in Russian). DOI: 10.20537/nd1101006.
14. Kuznetsov L, Zaslavsky GM. Passive particle transport in three-vortex flow. Phys. Rev. E. 2000;61(4):3777–3792. DOI: 10.1103/PhysRevE.61.3777.
15. Leoncini X, Kuznetsov L, Zaslavsky GM. Motion of three vortices near collapse. Physics of Fluids. 2000;12(8):1911–1927. DOI: 10.1063/1.870440.
16. Yim H, Kim SC, Sohn SI. Motion of three geostrophic Bessel vortices. Physica D: Nonlinear Phenomena. 2022;441:133509. DOI: 10.1016/j.physd.2022.133509.
17. Gröbli W. Spezielle Probleme über die Bewegung geradliniger paralleler Wirbelfäden. Vierteljahrsch. d. Naturforsch. Geselsch. 1877;22:129–165 (in German).
18. Novikov EA. Dynamics and statistics of a system of vortices. Sov. Phys. JETP. 1975;41(5): 937–943.
19. Velasco Fuentes OU, van Heijst GJF, van Lipzig NPM. Unsteady behaviour of a topography-modulated tripole. J. Fluid Mech. 1996;307:11–41. DOI: 10.1017/S002211209600002X.
20. Gudimenko AI, Zakharenko AD. Three-vortex motion with zero total circulation. Journal of Applied Mechanics and Technical Physics. 2010;51(3):343–352. DOI: 10.1007/s10808-010-0047-5.
21. Aref H. Stirring by chaotic advection. J. Fluid Mech. 1984;143:1–21. DOI: 10.1017/S002211 2084001233.
22. Govorukhin VN, Morgulis A, Yudovich VI, Zaslavsky GM. Chaotic advection in compressible helical flow. Phys. Rev. E. 1999;60(3):2788–2798. DOI: 10.1103/PhysRevE.60.2788.
23. Borisov AV, Mamaev IS, Ramodanov SM. Basic principles and models of dynamic advection. Dokl. Phys. 2010;55(5):223–227. DOI: 10.1134/S1028335810050058.
24. Ryzhov EA, Koshel KV. Global chaotization of fluid particle trajectories in a sheared two-layer two-vortex flow. Chaos. 2015;25(10):103108. DOI: 10.1063/1.4930897.
25. Koshel KV, Sokolovskiy MA, Davies PA. Chaotic advection and nonlinear resonances in an oceanic flow above submerged obstacle. Fluid Dynamics Research. 2008;40(10):695–736. DOI: 10.1016/j.fluiddyn.2008.03.001.
26. Aref H, Blake JR, Budišić M, Cardoso SSS, Cartwright JHE, Clercx HJH, El Omari K, Feudel U, Golestanian R, Gouillart E, van Heijst GF, Krasnopolskaya TS, Le Guer Y, MacKay RS, Meleshko VV, Metcalfe G, Mezić I, De Moura APS, Piro O, Speetjens MFM, Sturman R, Thiffeault JL, Tuval I. Frontiers of chaotic advection. Rev. Mod. Phys. 2017; 89(2):025007. DOI: 10.1103/RevModPhys.89.025007.
27. Govorukhin VN. Numerical study of dynamical system generated by CABC vector field. Izvestiya VUZ. Applied Nonlinear Dynamics. 2020;28(6):633–642 (in Russian). DOI: 10. 18500/0869-6632-2020-28-6-633-642.
28. Petrovskaja NV. Low-order dynamical models for vortical flows of inviscid fluid in square

area. Izvestiya VUZ. Applied Nonlinear Dynamics. 2009;17(6):159–172 (in Russian). DOI: 10.18500/0869-6632-2009-17-6-159-172.
29. Delbende I, Selçuk C, Rossi M. Nonlinear dynamics of two helical vortices: A dynamical system approach. Phys. Rev. Fluids. 2021;6(8):084701. DOI: 10.1103/PhysRevFluids.6.084701.
30. Sengupta TK, Singh N, Suman VK. Dynamical system approach to instability of flow past a circular cylinder. J. Fluid Mech. 2010;656:82–115. DOI: 10.1017/S0022112010001035.
31. Prants SV. Dynamical systems theory methods to study mixing and transport in the ocean. Physica Scripta. 2013;87(3):038115. DOI: 10.1088/0031-8949/87/03/038115.
32. Ryzhov EA, Koshel KV, Carton XJ. Passive scalar advection in the vicinity of two point vortices in a deformation flow. European Journal of Mechanics - B/Fluids. 2012;34:121–130. DOI: 10.1016/j.euromechflu.2012.01.005.
33. Govorukhin VN. Numerical analysis of the dynamics of distributed vortex configurations. Comput. Math. Math. Phys. 2016;56(8):1474–1487. DOI: 10.1134/S0965542516080078.
34. Govorukhin VN, Filimonova AM. Analysis of the structure of vortex planar flows and their changes with time. Computational Continuum Mechanics. 2021;14(4):367–376. DOI: 10.7242/1999-6691/2021.14.4.30.
35. Govorukhin VN. An extended and improved particle-spectral method for analysis of unsteady inviscid incompressible flows through a channel of finite length. Int. J. Numer. Meth. Fluids. 2023;95(4):579–602. DOI: 10.1002/fld.5163.
36. Metcalfe G, Lester D, Trefry M. A primer on the dynamical systems approach to transport in porous media. Transport in Porous Media. 2023;146(1–2):55–84. DOI: 10.1007/s11242-022-01811-6.
37. Borisov AV, Mamaev IS. Mathematical Methods in the Dynamics of Vortex Structures. Moscow-Izhevsk: Institute of Computer Science; 2005. 368 p. (in Russian).
38. Ziglin SL. Nonintegrability of a problem on the motion of four point vortices. Sov. Math. Dokl. 1980;21:296–299.
39. Aref H. Stability of relative equilibria of three vortices. Physics of Fluids. 2009;21(9):094101. DOI: 10.1063/1.3216063.
40. Kizner Z. Stability of point-vortex multipoles revisited. Physics of Fluids. 2011;23(6):064104. DOI: 10.1063/1.3596270.
41. Rott N. Three-vortex motion with zero total circulation. Zeitschrift für angewandte Mathematik und Physik ZAMP. 1989;40(4):473–494. DOI: 10.1007/BF00944801.
42. Arnold VI, Kozlov VV, Neishtadt AI. Mathematical Aspects of Classical and Celestial Mechanics. 2nd edition. Berlin, Heidelberg: Springer; 1997. 294 p. DOI: 10.1007/978-3-642-61237-4.
43. de la Llave R. A tutorial on KAM theory. In: Katok A, de la Llave R, Pesin Y, Weiss H, editors. Smooth Ergodic Theory and Its Applications. Rhode: American Mathematical Society; 2001. 133 p. DOI: 10.1090/pspum/069/1858536.
44. Govorukhin VN. On the choice of a method for integrating the equations of motion of a set of fluid particles. Comput. Math. Math. Phys. 2014;54(4):706–718. DOI: 10.1134/S0965542514040071.
45. Hairer E, Wanner G, Lubich C. Geometric Numerical Integration: Structure-Preserving Algorithms for Ordinary Differential Equations. Vol. 31 of Springer Series in Computational Mathematics. Berlin, Heidelberg: Springer; 2002. 515 p. DOI: 10.1007/978-3-662-05018-7.
46. Hairer E, Nørsett SP, Wanner G. Solving Ordinary Differential Equations I: Nonstiff Problems. Berlin, Heidelberg: Springer; 1987. 482 p. DOI: 10.1007/978-3-662-12607-3.
47. Verner JH. Numerically optimal Runge–Kutta pairs with interpolants. Numerical Algorithms. 2010;53(2–3):383–396. DOI: 10.1007/s11075-009-9290-3.

48. Prince PJ, Dormand JR. High order embedded Runge-Kutta formulae. Journal of Computational and Applied Mathematics. 1981;7(1):67–75. DOI: 10.1016/0771-050X(81)90010-3.
49. Govorukhin V. ode87 Integrator [Electronic resource]. MATLAB Central File Exchange. Retrieved February 28, 2023. Available from: https://www.mathworks.com/matlabcentral/fileexchange/3616-ode87-integrator.